



Universidad Autónoma  
de Madrid

**Biblos-e Archivo**  
Repositorio Institucional UAM

**Repositorio Institucional de la Universidad Autónoma de Madrid**  
<https://repositorio.uam.es>

Esta es la **versión de autor** del artículo publicado en:  
This is an **author produced version** of a paper published in:

Clay Minerals 52.3 (2017): 341-350

**DOI:** <https://doi.org/10.1180/claymin.2017.052.3.05>

**Copyright:** © 2017 The Mineralogical Society of Great Britain and Ireland

El acceso a la versión del editor puede requerir la suscripción del recurso  
Access to the published version may require subscription



62 materials and results indicated that this clay mineral is worth of further  
63 research for retention PAHs in order to add and complement novel functions  
64 in reactive barriers.

65

66 **Key words:** Organic Pollutants, Phenanthrene, Sepiolite, Stevensite,  
67 Adsorption, Isotherms

68

## 69 INTRODUCTION

70 The presence of emerging organic pollutants has become an issue of concern  
71 for a healthy and safe environment. Due to their potential carcinogenic and  
72 recalcitrant effects, the Environmental Protection Agency (EPA, 1980) and  
73 Water Framework Directive (2000/60/EC) have included PAHs in the list of  
74 priority pollutants. PAHs are generated during the incomplete combustion of  
75 fossil fuels and find their way into the soil and water via atmospheric fallout,  
76 urban run-off, municipal effluents, industrial effluents and oil spillage  
77 (Changchaivong & Khaodhiar, 2009). PHE is one of the most widespread  
78 PAHs with three fused benzene rings, often used as a model compound to  
79 study the fate of PAHs in contaminated soils (Jia *et al.*, 2012). PAHs  
80 dispersion and migration through waters and sediments depends on the  
81 interactions with the soil components. Adsorption to these surfaces is  
82 governed by the structural properties of soil particles like the presence of  
83 interlayers in clay minerals, high specific surface area (SSA), surface

84 conformation, density location of electric charge and type of exchangeable  
85 cations (Zhang *et al.*, 2011). Clays and clay minerals are considered one of  
86 the most reactive components of soil (Huang *et al.*, 2012). These are  
87 nanostructured materials or NPs (nanoparticles) capable of retaining organic  
88 compounds from aqueous phases and sediments (Brigatti *et al.*, 2006).  
89 Applications of clay minerals for non-polar ionic compounds (NOPCs)  
90 control involves cation saturation with organic or inorganic modification. Due  
91 to the fact that clay minerals are naturally hydrophilic, for instance, smectite  
92 modification with suitable organic molecules has been proved to increase  
93 their hydrophobicity (Lee & Tiwari, 2012). Exchange reactions with large  
94 organic cations enhances the surface hydrophobicity of clay materials, which  
95 enabled it an enhanced sorption capacity towards PAHs mainly by van der  
96 Waals forces and hydrogen bonding (Lagaly, Ogawab & Décány, 2006; Lee  
97 *et al.*, 1990). Additionally, cation modified clay minerals can adsorb a larger  
98 amounts of NOPCs like PHE (Jia *et al.*, 2015). These modified clays materials  
99 have shown a great potential as sorbents of PAHs. Nevertheless, in terms of  
100 NPOCs retention, few studies have focused on natural sepiolite (Cobas *et al.*,  
101 2014) and to our knowledge, there are not previous studies with stevensite,  
102 despite of the fact this type of smectite was previously studied for ionic  
103 organic compounds and metal trapping (Khalid *et al.*, 2011; Benhammou *et*  
104 *al.*, 2005a; Benhammou *et al.*, 2005b). Stevensite and sepiolite are  
105 magnesium rich clay minerals with low cation exchange and potential surface

106 for non-ionic interactions. (Lee *et al.*, 2004; Liu *et al.*, 2009). Additionally,  
107 stevensite and sepiolite are also attractive materials since they are widespread,  
108 generally easily mined, and relatively inexpensive. Their high SSA and  
109 volume of small pores enable them to adsorb significant amounts of PAHs.  
110 These properties make natural clay minerals to receive increasing attention in  
111 environmental protection issues (Churchman *et al.*, 2006).  
112 Currently, there is some debate about which mechanism governing the  
113 interaction between clay minerals and PAHs (McBride, 1994) and therefore,  
114 which is the suitable model to describe this interaction. One useful tool to  
115 approach adsorbate-adsorbent interaction mechanisms are adsorption  
116 isotherms. Hence, batch assays have been run in order to determinate the  
117 suitable isotherm. Previous studies found that Freundlich model provided the  
118 strongest correlation between sepiolite and PHE interaction (Cobas *et al.*,  
119 2014). Regarding to smectites, several works have reported the best fit for  
120 Freundlich model (Huang *et al.*, 1996, Zhang *et al.*, 2011), all of them  
121 according with physical attraction. On the opposite, Changchaivong &  
122 Khaodhilar (2009) found that the main adsorption mechanism is partitioning  
123 which is explained by a linear model. The use of permeable reactive barriers  
124 represents a widespread technology mostly studied for removal of inorganic  
125 compounds such as metals ions or nitrates. However, the interactions with  
126 NPOCs is in the early stages of development and the laboratory or field  
127 examples available for this type of pollutant remediation are limited. Then,

128 by means of obtaining adsorption isotherms, the aim of the present study was  
129 to (i) quantify the PHE adsorption capacity of stevensite and sepiolite; and  
130 (ii) to approach the main adsorption mechanisms and how the structural  
131 differences influence the behaviour of the selected materials within the  
132 context of clays minerals and other adsorptive materials found in the  
133 literature.

134 The results of the present work suggest the use of stevensite as material with  
135 potential for use in permeable reactive barriers due to its versatile capacity to  
136 retain polar and non-polar polluting compounds. Additionally, these materials  
137 are of low cost and have minimal environmental impact (Suárez & Garcia-  
138 Romero, 2012) compared to materials currently used like active carbon or  
139 artificially processed cation-modified clay minerals.

140

## 141 MATERIALS AND METHODS

### 142 *Phenanthrene*

143 PHE with a purity of 98% was obtained from Aldrich Chemistry  
144 Company. A primary methanol stock solution was prepared by dissolving an  
145 appropriate amount of solute in methanol and it was stored in the dark at 4  
146 °C. The use of methanol eliminates the need for lengthy shaking times to  
147 prepare PHE solutions and also because in the presence of methanol the  
148 solutions were stable for extended periods (Hundal *et al.*, 2001), while final

149 low methanol concentration achieved in batch assays (< 1%) do not modify  
150 the PHE sorption properties of sorbents (Weber & Huang, 1996;  
151 Changchaivong & Khaodhiar, 2009).

152

### 153 *Clay Minerals*

154         Stevensite and sepiolite materials were supplied by Tolsa SA (Spain)  
155 under the commercial names of MINCLEAR N100® (stevensite) and  
156 PANSIL® (sepiolite). Both clay minerals are quarried from the deposits of  
157 the Madrid Basin. MINCLEAR N100® presents at least 90 % wt grade of  
158 stevensite while PANSIL® presents above 90 % wt grade in sepiolite.

159 Clay minerals were characterized by X-ray diffraction (XRD) and by  
160 transmission electron microscopy (TEM) (Fig. 1a and 1b). XRD patterns were  
161 recorded using a  $\theta/2\theta$  X-PERT Panalytical® instrument with an X-  
162 CELERATOR detector (Cu K $\alpha$  monochromatic radiation). TEM micrographs  
163 were obtained using a JEOL 200FX microscope. Millimetre chip samples  
164 were indurated with a LR-White RESIN, then mounted and prepared as a thin  
165 section to be transferred to a TEM copper ring sample support (i.e., Warr &  
166 Nieto, 1998). Samples were thinned using ion beam equipment prior to  
167 observation.

168 MINCLEAR N100® contains illite impurities, dolomite, feldspar and quartz.  
169 Nevertheless, according to MINCLEAR N100® specifications, the stevensite

170 content is high as far as (hk0) asymmetric reflections dominate the pattern  
171 profile. Basal spacing Bragg reflections (00l) are very broad and are poorly  
172 developed.

173 The analyses confirmed the dominance of nanometre-sized particles. In  
174 sepiolite samples a typical fibrous morphology was observed (between 8 and  
175 10 nm of width and between 1 and 10  $\mu\text{m}$  in maximum dimension of length.  
176 Fig. 1b). They are grouped into parallel bundles, which creates an open  
177 porosity. Stevensite occurs as inter-aggregates with laminar structure with  
178 flakes less than 2 nm in thickness (two structural sheets; Fig. 1a).  
179 Additionally, the material characterization was complemented with SSA  
180 measurements by  $\text{N}_2$  adsorption through the BET method (Brunauer, Emmet,  
181 & Teller, 1938, in Web & Orr, 1997) using the porosimeter model Gemini V  
182 of Micromeritics®. The results showed a high external SSA ( $221 \pm 2 \text{ m}^2/\text{g}$  for  
183 MINCLEAR N100® samples and  $293 \pm 4 \text{ m}^2/\text{g}$  for PANSIL samples). These  
184 experimental measurements are consistent with those published by Cuevas *et*  
185 *al.* (1993): 250-280  $\text{m}^2/\text{g}$  for stevensite SSA and Suárez & Romero (2012):  
186 308  $\text{m}^2/\text{g}$  for sepiolite SSA analyses, which were provided by TOLSA S.A.  
187 (Spain) too from the same quarries.

188 Clay minerals sorption capacity was tested in batch assays. Sorption rate and  
189 equilibrium experiments were conducted at  $25 \pm 3^\circ \text{C}$ . These assays were  
190 performed in Erlenmeyer flasks (trademark SIMAX®) by mixing adsorbents:  
191 clay minerals / water ratios were 1:125 (w: w). Initially, 0.3 g of clay minerals



192 was suspended in 0.1 M NaNO<sub>3</sub> background electrolyte solution for ionic  
193 strength control. Subsequently, the pH conditions were adjusted at  $6 \pm 1$ .  
194 Finally, a desired amounts of stock solution were spiked. Ranging initial  
195 concentrations from 0.3 mg/L to 3.6 mg/l (supersaturated) of PHE were  
196 prepared.

197 In order to avoid PHE losses, flask reactors were sealed with aluminium foil.  
198 Additionally, blanks test without clay minerals were also prepared in the same  
199 way to account losses of PHE others than sorption by the clays. The samples  
200 were equilibrated on a reciprocating shaker (P. Selecta® Fuse) for 2 h at 120  
201 rpm in order to ensure completely homogenous mixing. After equilibration,  
202 the samples and controls were centrifuged for 10 min at 4500 rpm, then PHE  
203 concentrations in supernatant were analysed by UV-spectrophotometry at 254  
204 nm (Manoli & Samara 1999; Jia *et al.*, 2012). Finally, it is noteworthy to  
205 mention that the clay minerals deposited on the flask reactors during the  
206 centrifugation process were recovered, dried and stored for further studies.

207

208 *Data analysis.*

209 The amount of PHE adsorbed onto the adsorbent was calculated  
210 using the following equation:

211 
$$qe = \frac{Co - Ce}{m} V \quad (1)$$

212 where  $qe$  is mg of PHE adsorbed per g of clay mineral (solid phase-  
213 concentration).  $C_o$  and  $C_e$  are the initial concentration and final equilibrium  
214 concentration respectively (in mg/L),  $V$  is the volume of the solution (in L),  
215 and  $m$  is the mass of clay mineral used (expressed in g).

216 The data for the sorption of PHE by clay minerals were fitted by two sorption  
217 isotherm models: (i) the linear model:

$$218 \quad qe = K_D Ce \quad (2)$$

219 and (ii) the Freundlich model:

$$220 \quad qe = K_F Ce^n \quad (3)$$

221 where  $C_e$  is equilibrium solution concentration (mg/L) of PHE.  $K_D$  (equation  
222 2) is the linear distribution coefficient and  $K_F$  is the Freundlich coefficient.  
223 Both parameters provide the amount of PHE adsorbed per unit mass of  
224 sorbent [(mg/g) / (mg/mL)<sup>n</sup>] (sorption capacity). The Freundlich exponent,  $n$ ,  
225 is an empirical constant and representing a site energy heterogeneity index.  
226 The Freundlich model (equation 3) reflects heterogeneous sorption sites with  
227 a distribution of sorption energies.

228 To compare several types of sorbent materials, a derivation of the Freundlich  
229 model was used due to the limitations that this equation presents (Bowman &  
230 Sans, 1985). The Freundlich coefficient,  $K_F$ , has a limited use due to its  
231 inconsistent units, then previous works have removed the influence of  $n$  on  
232  $K_F$ . The dimensions of  $K_F$  can be made independent of the value of  $n$  by

233 modifying the Freundlich model and using the concept of reduced  
234 concentration. In an earlier paper by Carmo *et al.* (2001), the authors  
235 discussed in detail and step-by-step the derivation of the Freundlich model.  
236 Briefly,  $C_e$  is substituted for  $C_r$  (reduce concentration) in equation 3:

$$237 \qquad qe = K'_F C_r^n \qquad (4)$$

238 where  $C_r$  (dimensionless) is the ratio of  $C_e$  to the supercooled liquid-state  
239 solubility of PHE. The value of the supercooled liquid-state aqueous  
240 solubility of PHE is 5.902  $\mu\text{g/mL}$  at 25 °C. The  $K'_F$  is called the modified  
241 Freundlich coefficient and provides an index of sorption capacity. The values  
242 of  $K'_F$  can be used to compare directly the sorption characteristics of  
243 heterogeneous sorbents using equivalent Freundlich coefficients.

244 The sorbents compared were: K-hectorite, from Hundal *et al.* (2001). It was  
245 purchased from the Source Clays Repository of the Clay Minerals Society,  
246 while the Ca-smectite, selected from Zhang *et al.* (2011), was obtained from  
247 Beijing Ruizhx Tech Co., Ltd. These smectites were fractioned by  
248 sedimentation to collect  $< 2 \mu\text{m}$  fractions. Then, these fractions were saturated  
249 with  $\text{K}^+$  and  $\text{Ca}^{2+}$ , respectively, using chloride salts. After saturation process,  
250 the excess of salts were removed and finally they were freeze dried.

251 Additionally, non-porous alumina ( $\alpha\text{-Al}_2\text{O}_3$ ) and silica gel were compared  
252 too. Both sorbents were taken from Huang *et al.* (1996). Alumina was  
253 provided by Alfa Inc. and had particle diameters of approximately 1  $\mu\text{m}$  and

254 silica gel was provided by Davisil, Aldrich and was porous beads of 63-300  
255  $\mu\text{m}$  diameter.

256 Finally, all adsorption experimental data were fitted to mathematical  
257 adsorption models using ORIGIN PRO<sup>®</sup> 8 software.

258

## 259 RESULTS

### 260 *Stevensite and sepiolite adsorption isotherms*

261 The equilibrium adsorption isotherms were evaluated by plotting the  
262 solid-phase concentration ( $q_e$ ) against the liquid-phase concentration ( $C_e$ ).  
263 Freundlich and linear model showed virtually the same fit for PHE adsorption  
264 on clay minerals (Table 1). Both clays exhibited affinity for PHE, however  
265 higher sorption rates were found in stevensite measurements, in which the  
266 Freundlich parameters  $K_F$  and  $n$  presented are higher together with the  $K_D$   
267 value, belonging to linear model. The PHE uptake (Fig. 2a and Fig. 2b)  
268 concomitantly increased with PHE equilibrium concentration. Above PHE  
269 saturated aqueous equilibrium concentration around 1 mg/L (i.e., Fig. 2a)  
270 there was not possible to evaluate PHE solid adsorption due to PHE  
271 precipitation or volatilization (de Maagd *et al.*, 1998; Sawamura, 2000).

272

### 273 *Comparative by heterogeneous sorbent materials*



295 characterized by an initial slope that remains independent of adsorptive  
296 concentration until the maximum possible adsorption is achieved. This kind  
297 of isotherm can be produced by a proportional increase in the amount of  
298 adsorbing surface as the surface excess increases (Sposito, 2008). It is worth  
299 mentioning that the adjustment of isotherm results suggests an acceptable  
300 good fit for both models, but the limiting fact of PHE aqueous solubility do  
301 not allow to follow the isotherm bending up to higher concentrations and to  
302 decide which model is predominating.

303 It is currently under discussion which of the two mechanisms explains best  
304 the behaviour of highly hydrophobic compounds such as PHE on clay  
305 minerals. Using molecular models, Meleshyn & Tunega, 2011 have shown  
306 that the adsorption mechanism of PHE on montmorillonite in the presence of  
307 water is not significant. In addition, previous works conducted by  
308 Changchaivong & Khaodhiar (2009) using adsorption isotherms suggested  
309 that the main adsorption mechanism is partition, which is explained by a  
310 linear model. In this regard, repulsion strength between water molecules and  
311 PHE would cause the molecule displacement towards the hydrophobic  
312 mineral clay positions, and this would increase the entropy favouring a more  
313 stable energy state (Piatt *et al.*, 1996). Moreover, previous studies of PHE  
314 adsorption isotherms on clays have shown the best fit to the Freundlich model  
315 (Huang *et al.*, 1996, Zhang *et al.*, 2011). Also, it should be noted the ability  
316 of water to accommodate the hydrophobic compounds is highly dependent on

317 molecular size (McBride, 1994; de Maagd *et al.*, 1998; Churchman *et al.*,  
318 2006; Lee & Tiwari, 2012; Lagaly, Ogawab & Dékány, 2013). The data  
319 obtained in the present work showed a good fit for both models (Table 1),  
320 suggesting that either both mechanisms may offer an interpretation to the  
321 results.

322 Regarding to stevensite and sepiolite adsorption capacity, the data indicate  
323 that PHE was mostly adsorbed to stevensite since the Freundlich and linear  
324 model parameters  $K_F$ ,  $n$  and  $K_D$  presented are significantly higher for this clay  
325 mineral (Table 1; Fig 2a-b). The reason of the dissimilar behaviour of  
326 stevensite and sepiolite might be due to their structural and aggregation  
327 differences. Smectites have an interlayer thickness that may range from 0.2-  
328 0.4 nm, between ~1 nm 2:1 structural layers (dry), to several nm in wet  
329 conditions, measured between coherently stacked layers (quasicrystals,  
330 Hundal *et al.*, 2001; Fig. 4a). This may provide to planar PHE molecules high  
331 accessibility to the internal planar micropores surfaces. Regarding sepiolite  
332 structure, it has a fibrous morphology due to the periodic silica tetrahedral  
333 inversion in the tetrahedral sheets. This inversion implies the existence of  
334 channels whose dimensions hamper coupling PHE molecule. The dimensions  
335 of the channels pores are around 0.4 nm x 1.08 nm (Fig. 4b) (Tang *et al.*,  
336 2012; Suárez & Romero, 2012; Ahmed, Helmy & de Bussetti, 2008) whereas  
337 a PHE molecule has a size of 1 nm in aqueous solution (Huang *et al.*, 1996).  
338 Thus, sepiolite could not accommodate easily the PHE molecule inside the

339 channels based on size issues. Despite of organic compounds could be readily  
340 moved by water molecules, the van der Waals forces ( $\pi$ - $\pi$  interactions with  
341 siloxane surface, significant in large NPOC low solubility molecules; Lagaly  
342 *et al.*, 2013), can result in hydrophobic bonding type. Another critical  
343 parameter is the SSA. This value is a measure of the external SSA in sepiolite,  
344 but in expandable colloids such as stevensite, the measurements by the BET  
345 method underestimates the total specific particle surface. The N<sub>2</sub> gas, used in  
346 BET method measurements, only penetrates to a small portion of the regions  
347 of the interlayers, which is precisely where 80% of the total surface area  
348 (Bohn, 1993) is located. So that, at equal external SSA provided for the tested  
349 materials, stevensite compared to sepiolite, will exhibit larger planar surface  
350 sites available for adsorption.

351

352 *Comparison with heterogeneously sorbing materials. Modification of the*  
353 *Freundlich equation.*

354 The results obtained through the modified Freundlich equation are in  
355 agreement with the results and conclusion of the literature presented. The  
356 affinity of K-saturated smectites for some NOPCs can be similar and even  
357 larger than affinity of soil organic matter (Yuan *et al.*, 2013). In the same way,  
358 uptake of NOPCs by expanding clay minerals as smectites is enhanced when  
359 the saturating cations are weakly hydrated and provide larger adsorption  
360 areas. The comparison based on modified Freundlich equation suggests that



361 stevensite might has sorption capacities similar to those of cation-modified  
362 clay minerals: Ca-smectite and K-Hectorite. In any case, the highest  
363 adsorption capacity provided by the smectites group (regarding the  
364 modification of the Freundlich parameters and the shape of isotherms (Table  
365 2; Fig.3), could be due to the presence of hydrophobic areas with strong  
366 affinity to non-polar compounds attributable to the presence of laminar  
367 siloxane groups in the basal planes (Cruz-Guzmán, 2007). This relative  
368 hydrophobicity of the smectites surface is influenced mainly by type of layer  
369 and location of the charge, either predominantly tetrahedral or octahedral  
370 (Laird, 1999). Moreover, it is known that in aqueous solutions, platelets of  
371 clay crystal favour the formation of a fine network of quasicrystals with a  
372 large number of microspores to retain PHE. The PHE adsorption capacity  
373 increase in the cation-modified minerals when zeta potential of these minerals  
374 approached neutral (Zhang *et al.*, 2011). Likewise have been investigated that  
375 the adsorption increase as the layer charge of the clay mineral decrease  
376 (Sheng *et al.*, 2002). The association of NOPCs and clay minerals may be  
377 also enhance by the van der Walls interactions between the compounds and  
378 the basal siloxane surface of clay minerals above mentioned. Similarly, Qu *et*  
379 *al.* (2011) have suggested that the adsorption to montmorillonite is affected  
380 by  $n-\pi$  electron donor-acceptor interactions between the compound and the  
381 siloxane oxygens ( $n$ -donors) of the clay mineral. However, in this study, it is  
382 point out that stevensite was not modified with any cation so as to enhance its

383 potential interactions with hydrophobic compounds, however this type of clay  
384 mineral showed a high adsorption capacity too. The stevensite are attractive  
385 in comparison with modified clay minerals because they are widespread,  
386 easily mined, and relatively inexpensive. In addition, stevensite are naturally  
387 occurring materials, non-toxic, and the results presented here, suggest a  
388 considerable capacity for controlling PHE. Besides stevensite have properties  
389 such as colloidal behaviour, and swelling capacity, the underlying reason  
390 might be that the stevensite have characteristics related to an extremely low  
391 cation exchange capacity generated by a deficiency of octahedral cations due  
392 to the absence of isomorphic substitutions (De Santiago *et al.*, 2000; Cuevas  
393 *et al.*, 1993). Moreover, in this work it is showed that setevensite has  
394 nanometre-size particles with a very low crystal thickness and high external  
395 specific surface in their structure, as suggest experimental results obtained by  
396 TEM and SSA analyses.

397 Regarding the comparison with other type of materials, the smooth and planar  
398 surface of the smectite inter-quasicrystals favoured PHE adsorption. Indeed,  
399 rough or cylindrical surface as silica gel or alumina appear less effective for  
400 molecule attachment (Huang *et al.*, 1996). Despite the fact that all of these  
401 materials have average pore diameters greater than the molecular length of  
402 PHE, these pores are much less efficient with respect to PHE sorption.

403

## 404 CONCLUSIONS

405 The present work provides promising results in support of the use of  
406 stevensite (smectites group) as, for instance, component of a reactive  
407 permeable barrier for retention of non-polar organic pollutants. The smectites  
408 modified with inorganic cations have shown properties that allow them to  
409 retain large amounts of PHE, a hazardous organic pollutant, but natural  
410 stevensite present advantages over other sorbents such as the easy availability  
411 in significant amounts as it is known in the Madrid Basin and its relatively  
412 inexpensive. The adsorption capacity and the mechanisms involved were  
413 discussed in terms of the assumption of the Freundlich model in order to  
414 compare with other similar adsorbents and between stevensite and sepiolite.  
415 Since hydrophobic interactions and planar inter-quasicrystal accommodation  
416 are likely to be the dominant mechanism of PHE adsorption by stevensite,  
417 sepiolite offered less available sites for adsorption.

418 The adsorption capacity of clay minerals should be accomplished with  
419 complementary analytical measurements and experiments such as column  
420 assays where it would be very interesting to carry out experiments with higher  
421 PHE concentrations using solvents that avoid the PHE losses in order to  
422 achieve more complete isotherms up to higher PHE concentrations.

423 Additionally, in further experiments, it is envisaged to characterize the  
424 recovered clay minerals from the centrifugation stage (clay minerals  
425 deposited on the flasks reactors) as well as to test the regeneration of the  
426 sorbents.

427

428

## ACKNOWLEDGEMENTS

429

To E. Eymar and C. García Delgado for their support in the research team.

430

This work has been economically supported by Ministry of Economy and

431

Competitiveness of Spain (CTM2013-47874-C2-2-R).

432

- 434 Ahmed K., Helmy & Silvia G. de Bussetti. (2008) The surface properties of  
435 sepiolite. *Applied Surface Science*, **255**, 2920-2924.
- 436 Benhammou A., Yaacoubi A., Nibou L. & Tanouti B. (2005) Study of the  
437 removal of mercury (II) and chromium (VI) from aqueous solutions by  
438 Moroccan stevensite. *Journal of Hazardous Materials*, **117**, 243-249.
- 439 Benhammou A., Yaacoubi A., Nibou L. & Tanouti B. (2005) Adsorption of  
440 metal ions onto Moroccan stevensite: kinetic and isotherm studies. *Journal*  
441 *of Colloid and Interface Science*, **282**, 320-326.
- 442 Bohn H., McNeal B. & Oconor G. (1993) *Química del suelo*, pp. 147-148.  
443 Limusa, México, D.F.
- 444 Bowman B.T. & Sans W.W. (1985) Partitioning behaviour of insecticides in  
445 soil-water systems: I. Adsorbent concentration effects 1. *Journal*  
446 *Environment Quality*, **14**, 265.
- 447 Brigatti M.F., Galán E. & Theng B.K.G. (2006) Structures and mineralogy of  
448 clay minerals. Pp.19-85 in: *Handbook of Clay Science* (F. Bergaya, B.K.G.  
449 Theng & G. Lagaly, editors). Elsevier, Amsterdam.
- 450 Carmo A., Hundal L. & Thompson M. (2000) Sorption of Hydrophobic  
451 Organic Compounds by Soil Materials: Application of Unit Equivalent  
452 Freundlich Coefficients. *Environmental Science & Technology*, **34**, 4363-  
453 4369.
- 454 Changchaivong S. & Khaodhiar S. (2009) Adsorption of naphthalene and  
455 phenanthrene on dodecylpyridinium-modified bentonite. *Applied Clay*  
456 *Science*, **43**, 317-321.
- 457 Churchman G.J., Gates W.P., Theng B.K.G & Yuan G. (2013) Clays and  
458 Clays Minerals for Pollution Control. Pp.625-675 in: *Handbook of Clay*  
459 *Science* (F. Bergaya, B.K.G. Theng & G. Lagaly, editors). Elsevier,  
460 Amsterdam
- 461 Cobas M., Ferreira, L., Sanromán M.A. & Pazos M. (2014) Assesment of  
462 sepiolite as a low-cost adsorbent for phenanthrene and pyrene removal:  
463 Kinetic and equilibrium studies. *Ecological Engineering*, **70**, 287-294.
- 464 Cruz-Guzmán M. (2007) *La contaminación de los suelos y aguas. Su*  
465 *prevención con nuevas sustancias naturales*, pp. 82-83. Universidad de  
466 Sevilla, Sevilla.

- 467 Cuevas J., De La Villa R., Ramirez, S., Petit S., Meunier A. and Leguey S.  
 468 (2003) Chemistry of Mg Smectites in Lacustrine Sediments from the  
 469 Vicalvaro Sepiolite Deposit, Madrid Neogene Basin (Spain). *Clays Clay*  
 470 *Miner*, **51**, 457-472.
- 471 Cuevas, J., Pelayo, M., Rivas, P. y Leguey, S. (1993). Characterization of  
 472 Mg-Clays from the Neogene of the Madrid Basin and their potential as  
 473 backfilling and sealing material in high level nuclear waste disposal.  
 474 *Applied Clay Science*, **7**, 383-406
- 475 de Maagd P., ten Hulscher D., van den Heuvel H., Opperhuizen A. & Sijm D.  
 476 (1998) Physicochemical properties of polycyclic aromatic hydrocarbons:  
 477 aqueous solubilities, n-octanol/water partition coefficients, and henry's  
 478 law constants. *Environmental Toxicology and Chemistry*, **17**, 251.
- 479 De Santiago C.; Suárez M.; Garcia Romero E. & Doval M. (2000) Mg-rich  
 480 smectite "precursor" phase in the Tagus Basin, Spain. *Clays and Clay*  
 481 *Minerals*, **48**, 366-373.
- 482 EPA. 1980. Water quality criteria document for polynuclear aromatic  
 483 hydrocarbons. Environmental Protection Agency, Office of Health and  
 484 Environmental Assessment, Environmental Criteria and Assessment  
 485 Office, United States.
- 486 EU. 2000. Directive 2000/60/EC of the European Parliament and of the  
 487 council of 23 October, 2000. Establishing a framework for community  
 488 action in the field of water policy. European Union.
- 489 Huang P., Li, Y. & Sumner M. (2012) *Handbook of soil sciences*. Pp. 20-48  
 490 in: 2nd edition. CRC Press, Boca Raton, Fla.
- 491 Huang W., Schallautman M.A. & Weber W.J. (1996) A Distributed Reactivity  
 492 Model for Sorption by Soils and Sediments. 5. The Influence of Near-  
 493 Surface Characteristics in Minerals Domains. *Environmental Science &*  
 494 *Technology*, **30**, 2993-3000.
- 495 Hundal L.S., Thompson M.L., Laird D.A. & Carmo A.M. (2001) Sorption of  
 496 phenanthrene by reference smectite. *Environmental Science &*  
 497 *Technology*, **35**, 3456-3461.
- 498 Jia H., Zhao J., Fan X., Dilimulati K. & Wang, C. (2012) Photodegradation  
 499 of phenanthrene on cation-modified clays under visible light. *Applied*  
 500 *Catalysis B: Environmental*, **123–124**, 43– 51.
- 501 Jia H., Li L., Chen H., Zhao Y., Li X., Wang C. (2015) Exchangeable cations-  
 502 mediated photodegradation of polycyclicaromatic hydrocarbons (PAHs)

- 503 on smectite surface under visible light. *Journal of Hazardous materials*,  
504 **287**, 16-23.
- 505 Khalid E., Laachacha A., Alaouib A. & Azzic M. (2011) Removal of methyl  
506 violet from aqueous solution using a stevensite-rich clay from Morocco.  
507 *Applied Clay Science*, **54**, 90-96.
- 508 Lagaly, G, Ogawa & M, Décány, I. (2006) Clay minerals organic interaction.  
509 Pp.309-359 in: *Handbook of Clay Science* (F. Bergaya, B.K.G. Theng &  
510 G. Lagaly, editors). Elsevier, Amsterdam.
- 511 Lagaly G, Ogawa & Décány M.I. (2013) Clay minerals organic interaction.  
512 Pp.425-505 in: *Handbook of Clay Science*, **2**, (F. Bergaya & G. Lagaly,  
513 editors). Elsevier, Amsterdam.
- 514 Laird D.A. (1999) Layer charge influences on the hydration of expandable  
515 2:1 phyllosilicates. *Clays and Clay Minerals*, **47**, 630-636.
- 516 Lee J.F., Mortland M.M., Chiou C.T., Kile D.E & Boyd S.A. (1990).  
517 Adsorption of benzene, toluene, and xylene by two  
518 tetramethylammonium-smectites having different charge densities. *Clays  
519 and Clay Minerals*, **38**, 113–120.
- 520 Lee S.Y., Kim S.J., Chung S.Y., & Jeong C.H. (2004) Sorption of  
521 hydrophobic organic compounds onto organoclays, *Chemosphere*, **55**,  
522 781-785.
- 523 Lee S.M. & Tiwari D. (2012) Organo and Inorgano-Organo-Modified Clays  
524 in the Remediation of Aqueous Solutions: An Overview. *Applied Clay  
525 Science*, **59-60**, 84–102
- 526 Liu R., Frost R.L., Martens W.N. (2009) Near infrared and mid infrared  
527 investigations of adsorbed phenol on HDTMAB organoclays. *Materials  
528 Chemistry and Physics*, **113**, 707–713.
- 529 Manoli E. & Samara C. (1999) Polycyclic aromatic hydrocarbons in natural  
530 waters: sources, occurrence and analysis. *TrAC Trends in Analytical  
531 Chemistry*, **18**, 417-428.
- 532 McBride M. (1994) *Environmental Chemistry of Soil*, pp. 3-7; pp. 372-379  
533 Oxford University Press. New York.
- 534 Meleshyn A. & Tunega D. (2011) Adsorption of phenanthrene on Na-  
535 montmorillonite: A model study. *Geoderma*, **169**, 41–46.
- 536 Piatt J., Backhus D., Capel P. & Eisenreich S. (1996) Temperature-Dependent  
537 Sorption of Naphthalene, Phenanthrene, and Pyrene to Low Organic

- 538 Carbon Aquifer Sediments. *Environmental Science & Technology*, **30**,  
539 751-760.
- 540 Qu, X.L., Zhang, Y.J., Li, H., Zheng, S.R., Zhu, D.Q. (2011) Probing the  
541 specific sites on montmorillonite using nitroaromatic compounds and  
542 hexafluorobenzene. *Environ. Sci. Technol.* **45**, 2209–2216.
- 543 Rutherford D., Chiou C.T & Kile D.E. (1992) Influence of soil organic matter  
544 composition on the partition of organic compounds. *Environmental*  
545 *Science & Technology*, **26**, 336-340.
- 546 Sawamura S. (2000) Pressure Dependence of the Solubilities of Anthracene  
547 and Phenanthrene in Water at 25°C. *Journal of Solution Chemistry*, **29**,  
548 N°4.
- 549 Sheng G.Y., Johnston C.T., Teppen B.J., Boyd S.A. (2002) Adsorption of  
550 dinitrophenol herbicides from water by montmorillonites. *Clays and Clay*  
551 *Minerals*, **50**, 25–34.
- 552 Sposito G. 1989. *The Chemistry of Soils*, pp. 198-199. Oxford University.  
553 New York.
- 554 Suárez M., García-Romero E. (2012) Variability of the surface properties of  
555 sepiolite. *Applied Clay Science*. **67–68**, 72 – 82.
- 556 Tang Q., Wang F., Tang M., Liang J. & Ren C. (2012) Study on Pore  
557 Distribution and Formation Rule of Sepiolite Mineral Nanomaterials.  
558 *Journal of Nanomaterials*, **2012**, 1-6.
- 559 Warr, L.N., Nieto, F. (1998). Crystallite thickness and defect density of  
560 phyllosilicates in low-temperature metamorphic pelites: a TEM and XRD  
561 study of clay mineral crystallinity-index standards. *The Canadian*  
562 *Mineralogist*, **36**, 1453-1474.
- 563 Webb P.A., Or C. (1997) *Analytical methods in fine particle technology*, p.  
564 301. Micromeritics Instruments Corporation.
- 565 Weber W. J.; Huang W. (1996). A Distributed Reactivity Model for Sorption  
566 by Soils and Sediments. 4. Intraparticle Heterogeneity and Phase-  
567 Distribution Relationships under Non equilibrium Conditions. *Environtal*  
568 *Science Technology*, **30**, 881-888.
- 569 Yuan G.D., Theng B.K.G., Churchman G.J., & Gates, W.P. (2013) Clays and  
570 Clay Minerals for Pollution Control. Pp 587-644 in: *Developments in Clay*  
571 *Science. Volume 5A* (F. Bergaya & G. Lagaly, editors). Elsevier,  
572 Amsterdam.



573     Zhang L., Luo, L. & Zhang S. (2011) Adsorption of phenanthrene and 1,3-  
574         dinitrobenzene on cation-modified clay minerals. *Colloids and Surfaces*  
575         *A: Physicochemical and Engineering Aspects*, **377**, 278-283.  
576

## FIGURES AND TABLES

- TABLE 1. Sepiolite and stevensite parameters of Freundlich and linear models obtained after adjustment.  $K_F$ : Freundlich coefficient.  $n$ : Freundlich exponent.  $R^2$ : Coefficient of determination.  $RMSE$ : Root Mean Square Error.  $K_D$ : Partition coefficient.
- TABLE 2. Modified Freundlich coefficient ( $K'_F$ ) obtained from selected materials.
- FIG. 1. XRD patterns and TEM micrographs of the clay minerals: (a) stevensite; (b) sepiolite. Sep: sepiolite, Ill: illite; fNa/fK: sodium and potassium feldspars; PhySi: Phyllosilicates; dol: dolomite; Qtz: quartz.
- FIG. 2. Stevensite (a) and sepiolite (b) adsorption isotherms. The solid lines represent the fit to linear model (eq. 2) model while dash dot line represent the fit to Freundlich model (eq. 3) to the sorption data using analysis module of OriginPro® 8 software.
- FIG. 3. Adsorption isotherms of the selected materials. Lines show the fit to modified Freundlich model (eq. 4) to the sorption data using nonlinear regression curve module of OriginPro® 8 software. The scale that relates alumina and silica gel concentration adsorbed is the Y-axis at the right hand side of the Figure 3. Ca-smectite, stevensite, K-hectorite and sepiolite are related to right Y-axis.
- FIG. 4. Geometric structural and aggregation mode constraints taken into account in the adsorption of PHE. Figure 4a. Accommodation of PHE between planar quasicrystals formed by 2:1 stacked layers. Black circles are exchangeable cations positions dispersed due to the low cation exchange capacity (After Hundal *et al.*, 2001). Figure 4b: structure of sepiolite and channel dimensions.

608 TABLE 1.

		Sepiolite	Stevensite
Freundlich model $q_e = k_F C_e^n$	$K_F$	$0.59 \pm 0.04$	$1.87 \pm 0.04$
	$n$	$0.79 \pm 0.06$	$0.99 \pm 0.03$
	$R^2$	0.92	0.95
	$RMSE$	0.04	0.11
Linear model $q_e = k_D C_e$	$K_D$	$0.56 \pm 0.03$	$1.86 \pm 0.05$
	$R^2$	0.89	0.95
	$RMSE$	0.04	0.10

609

610

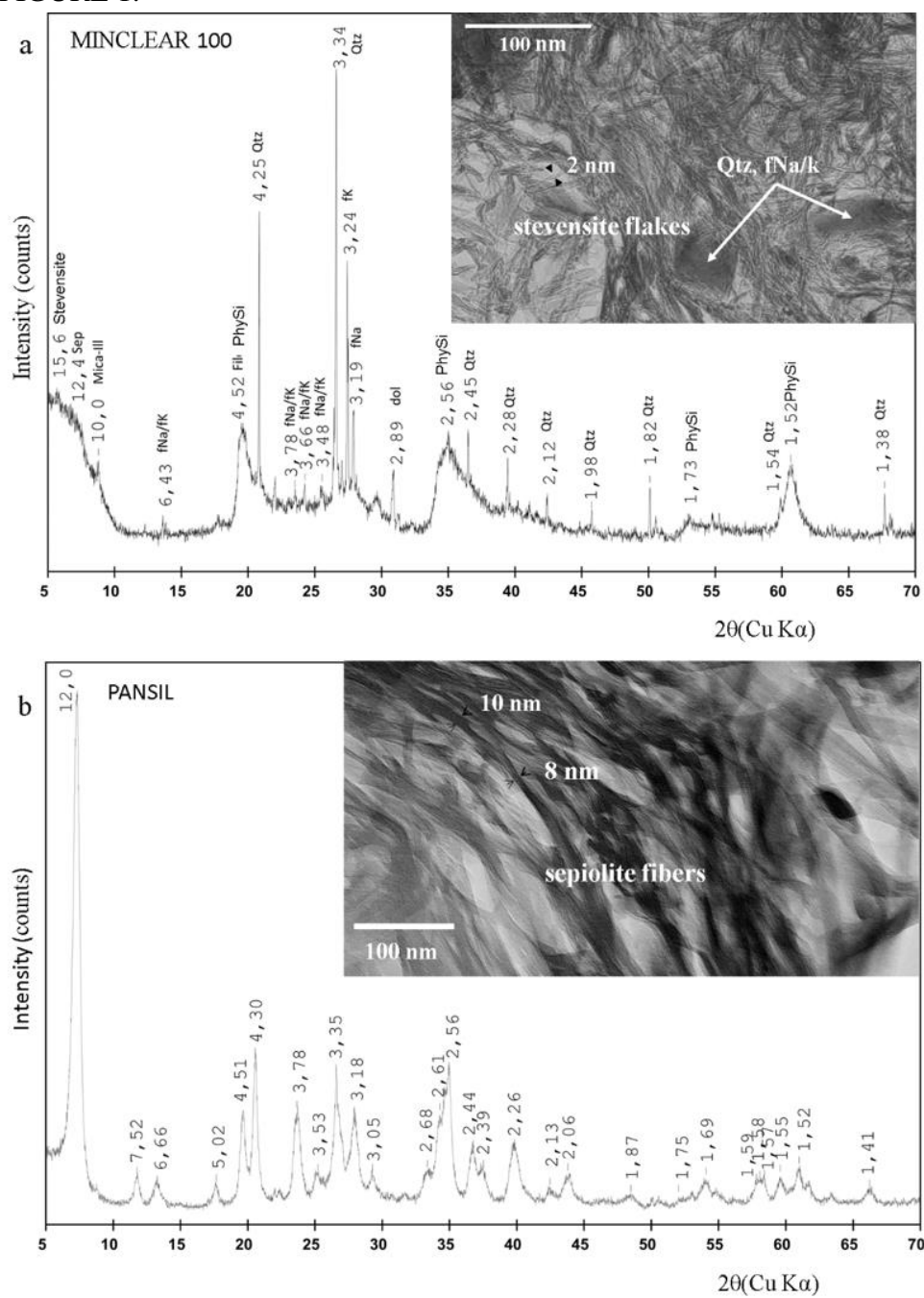
611 TABLE 2.

Adsorbent materials	$K'_F(\mu\text{g/g})$
alumina	$24.40 \pm 0.01$
silica gel	$543 \pm 49$
stevensite	$26878 \pm 1796$
Ca-smectite	$2044.01 \pm 0.08$
K-hectorite	$9282 \pm 680$
sepiolite	$108.45 \pm 0.12$

612

613

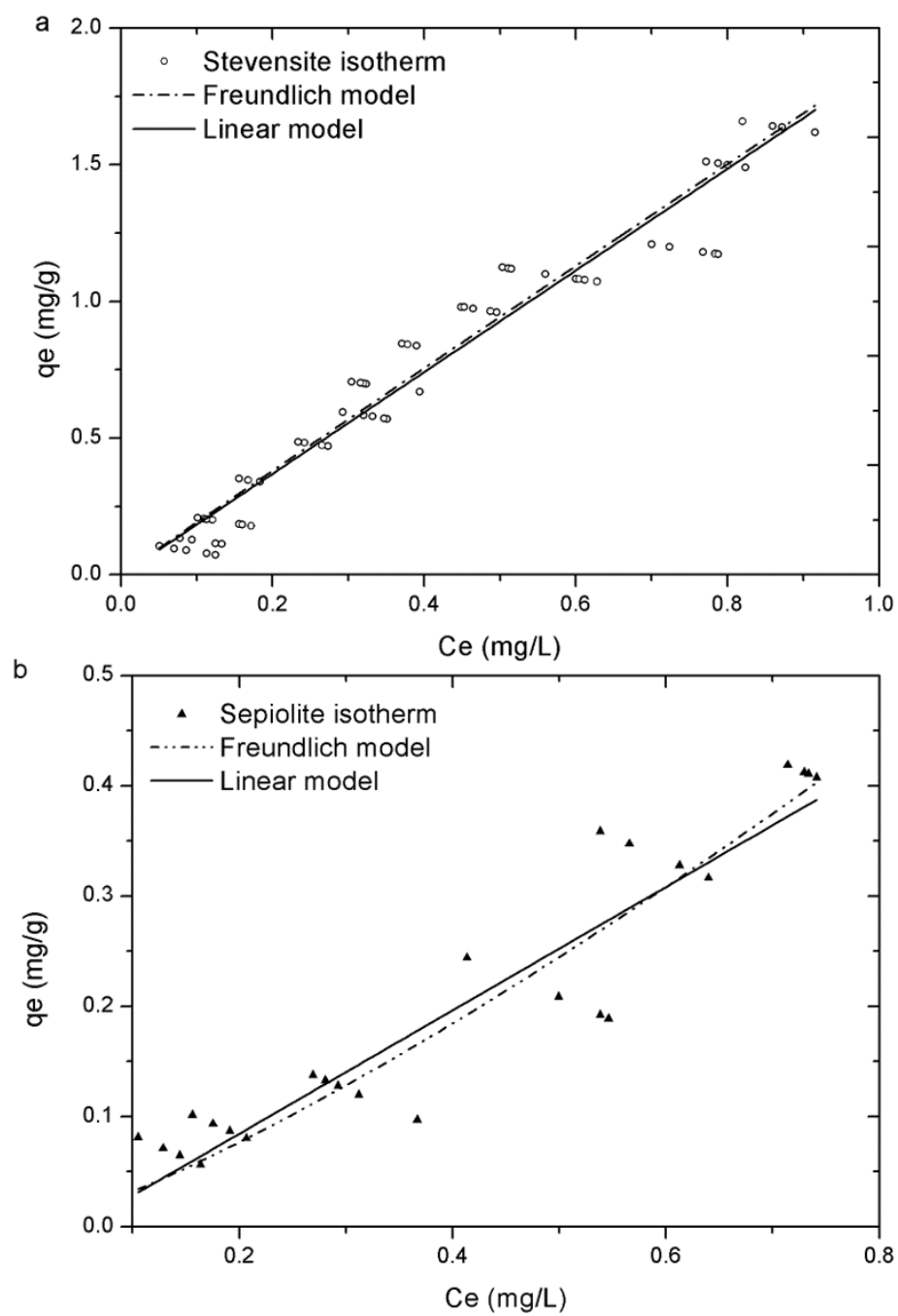
614 FIGURE 1.



615

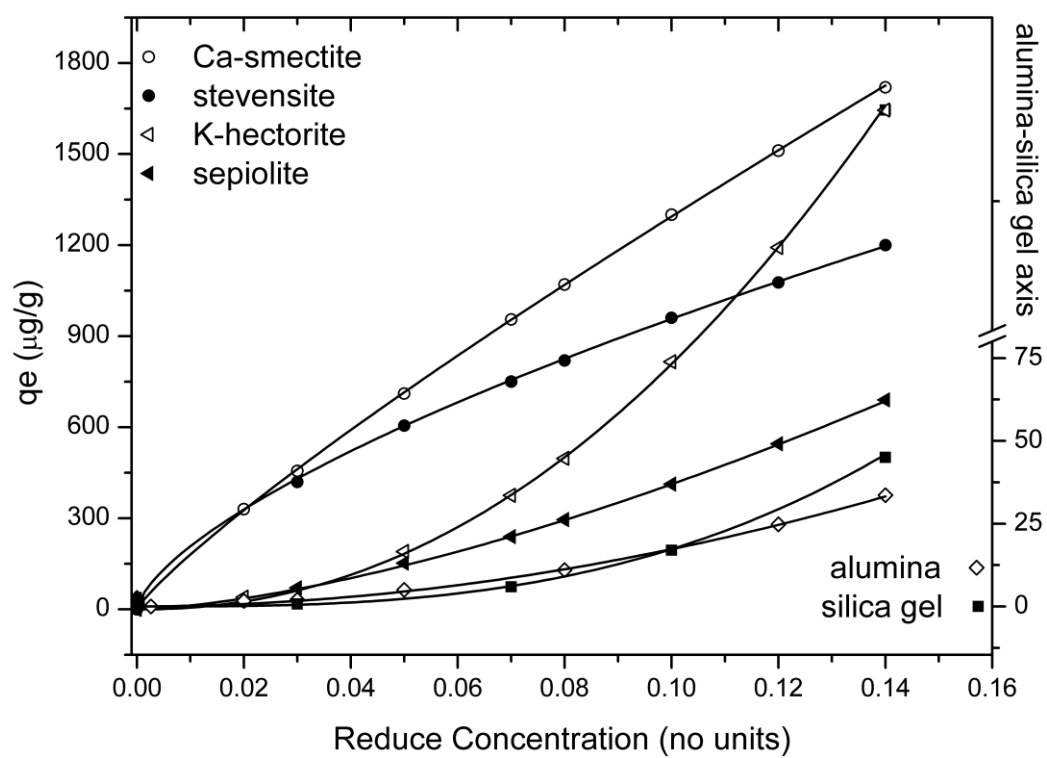
616

617 FIGURE 2.



618

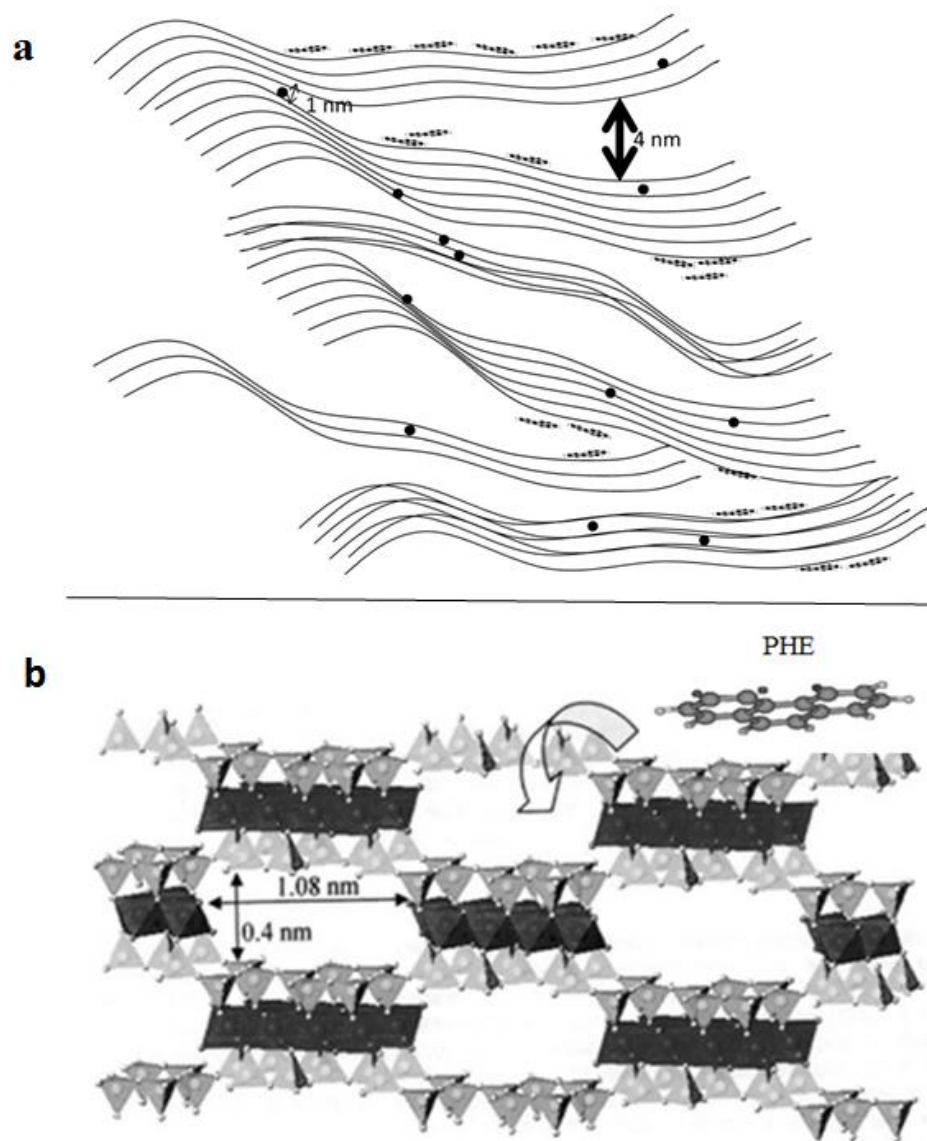
619 FIGURE 3.



620

621

622 FIGURE 4.



623